Biosensors and Bioelectronics 128 (2019) 166–175

Contents lists available at ScienceDirect

Biosensors and Bioelectronics

journal homepage: www.elsevier.com/locate/bios

Dielectrophoresis-based filtration effect and detection of amyloid beta in plasma for Alzheimer's disease diagnosis

Hye Jin Kim[a], Dongsung Park[a,b], Seung Yeop Baek[c], Seung-Hoon Yang[d], YoungSoo Kim[c], Sang Moo Lim[e], Jinsik Kim[f,*], Kyo Seon Hwang[a,*]

[a] Department of Clinical Pharmacology and Therapeutics, College of Medicine, Kyung Hee University, Seoul 02447, Republic of Korea
[b] School of Biomedical Engineering, College of Health Science, Korea University, Seoul 02841, Republic of Korea
[c] Integrated Science and Engineering Division, Department of Pharmacy, and Yonsei Institute of Pharmaceutical Sciences, Yonsei University, Incheon 21983, Republic of Korea
[d] Systems Biotechnology Research Center, Korea Institute of Science and Technology, Gangneung 25451, Republic of Korea
[e] Department of Neurology of Korea Cancer Center Hospital, Seoul 01812, Republic of Korea
[f] Department of Medical Biotechnology, College of Life Science and Biotechnology, Dongguk University, Seoul 04620, Republic of Korea

ARTICLE INFO

Keywords:
Dielectrophoresis
Filtration effect
Alzheimer's disease
Plasma-based diagnosis

ABSTRACT

The filtration effect improves the impedance change through specific binding of target molecules in plasma, and decreases this change by nonspecific binding of matrix factors in plasma (i.e., matrix effect). A difference in dielectrophoresis (DEP) forces applied to target molecules and matrix factors causes the filtration effect. An optimized DEP force affects target molecules, which remain in the reaction region of an interdigitated microelectrode (IME) sensor. Various matrix factors, which are larger than the target molecules, are influenced by a strong DEP force and are filtered out of the reaction region. To demonstrate the filtration effect, the matrix effect was confirmed in standard plasma and in phosphate-buffered saline, based on the detection of amyloid beta (Aβ), an Alzheimer's disease (AD)-associated peptide. The filtration effect was verified using the matrix effect factor (MEF), which was calculated from the impedance change values in different detection environments. In standard plasma, the MEF value decreased by approximately 78.12%, and in buffer with heterogeneous Aβ, by approximately 75.43%. Plasma from patients with AD and normal controls (NCs) was analyzed using the value of the impedance change by the filtration effect. The impedance change was enhanced approximately 1.52 ± 0.03-fold in AD plasma, but declined approximately 0.90 ± 0.03-fold in NC plasma. This difference tendency by the filtration effect was the disease evaluation index and used as an important criterion that distinguished between the AD and NC plasma. Plasma-based AD diagnosis may be possible, based on the filtration effect.

1. Introduction

Severe diseases are caused by biomolecules such as misfolded and aggregated proteins in biofluids (Dobson, 2003; Ross and Poirier, 2004). Information regarding biomolecules such as their presence or their concentration is used as a critical indicator to define a disease or to determine its progression, respectively (Rifai et al., 2006). To define diseases by using biomolecules, biofluids such as blood, saliva, and urine are generally utilized because samples are easily obtained (Herr et al., 2007; Tripathi et al., 2018). Therefore, the detection of extremely low concentrations of biomolecules in biofluids may have a significant implication for an early preclinical diagnosis. Most biomolecules at the early stage of diseases exist in biofluids at extremely low concentrations. However, detecting biomolecules in biofluids is extremely difficult to determine because of the requirement of high sensitivity and selectivity in detection methods for a target molecule. Several state-of-the-art technologies for high-sensitivity biomarker detection have been successfully developed such as nanostructured engineering (Soleymani et al., 2011), molecular engineering, modified deoxyribonucleic acid (DNA) probes (Gao et al., 2018), and DNA nanostructures (Wen et al., 2012). In general, biofluids that contain target biomolecules also include various nontarget biomolecules such as thrombin (Arya et al., 2011), transferrin (Al-Mashikhi and Nakai, 1988; Arya et al., 2011), immunoglobulin G1 (Al-Mashikhi and Nakai, 1988; Arya et al., 2011), and fibrinogen (Arya et al., 2011). This coexistence causes the matrix effect. These nontarget molecules interfere with the

* Corresponding authors.
E-mail addresses: lookup2@dongguk.edu (J. Kim), k.hwang@khu.ac.kr (K.S. Hwang).

https://doi.org/10.1016/j.bios.2018.12.046
Received 17 October 2018; Received in revised form 13 December 2018; Accepted 21 December 2018
Available online 02 January 2019
0956-5663/

detection of target molecules (De et al., 2009). Thus, the accuracy and precision of a target molecule's detection are expected to be low (De et al., 2009; Johansson and Hellenas, 2004), even if a highly sensitive detection method for target molecules is accomplished.

Various methods that reduce nonspecific binding of matrix factors have been used to improve the selectivity of a sensor. Typical approaches are as follows: using a receptor with a beacon that emits a signal only when the receptor interacts with specific molecules (Du et al., 2005); using a receptor with high affinity (Salazar and Strittmatter, 2017); or using a blocking agent such as Tween 20 and bovine serum albumin to reduce nonspecific binding (Batteiger and Jones, 1982; Jeyachandran et al., 2010). Moreover, physical filtration through various microstructures and a microfluidic channel have been used to alleviate the nonspecific binding of matrix factors (Choi et al., 2007; Gorkin et al., 2010). However, receptor-based approaches have a great disadvantage in that they act only on specifically engineered receptors, and the blocking agent-based approach may increase the complexity of an experiment or the blocking agents themselves may cause changes in the sensor. In addition, physical filtration involves the potential risk of removing the target molecules with matrix factors. Therefore, a method is needed that can be universally used and that reduces nonspecific binding without using physical removal while maintaining the simplicity of the experimental procedure.

Dielectrophoresis (DEP) is simple to apply and can be used for various receptors. Therefore, it is a promising candidate technique that can be used to increase the sensitivity of a sensor. Chuang et al. (2016) proposed an ultrasensitive and real-time impedance-based immunosensor by manipulating a nanoprobe with DEP force. Sharma et al. (2016) demonstrated a rapid, label-free, and highly sensitive single-walled carbon nanotube immunosensor by utilizing the concentration effect by DEP force. Our research group has also demonstrated that DEP improves the sensitivity of a sensor (Kim et al., 2016). In a previous study, we detected beta-amyloid (Aβ), a representative marker causing Alzheimer's disease (AD) (Hardy and Selkoe, 2002; Murphy and LeVine, 2010), at sub-femtogram per milliliter concentrations in phosphate-buffered saline (PBS). However, these results were obtained by applying one aspect of the DEP effect (i.e., the concentration effect).

In this study, the nonphysical filtration effect due to a local electric field (E-field) gradient change by DEP reduced the level of matrix factors in biofluids, and thereby allowed the detection of the target molecules. This effect allows biomolecules in plasma to filtrate according to size: the target protein binds to its antibody in the reaction region. However, in the plasma, biomolecules of sizes different from that of the target protein (i.e., matrix factors) are expelled from the region, thereby reducing the matrix effect. The filtration effect was demonstrated by measuring the impedance change in the sensor caused by the reaction of Aβ monomers in an optimized DEP condition, which was demonstrated in our previous study (Choi et al., 2007). Furthermore, to express the influence of the filtration effect more clearly, we defined and calculated the matrix effect factor (MEF). An interdigitated microelectrode (IME) sensor was used, and the filtration effect was verified in PBS and in standard plasma. Approximately 78.12% MEF was decreased by the filtration effect. This reduction discriminated between two types of plasma samples: plasma from patients with AD and plasma from the normal controls (NCs) (for each group, n = 10). The impedance change in the plasma sample from patients with AD was mostly increased by the filtration effect, whereas the changes in the NC plasma were very minute. This difference was indicated as the disease evaluation index, and the average value of the indexes were (expressed as the mean ± the standard deviation) approximately 1.52 ± 0.03 and 0.90 ± 0.03 in plasma samples extracted from patients with AD and from the NCs, respectively ($p < 0.001$; one-way analysis of variance [ANOVA]). Our study demonstrated that the filtration effect caused by the DEP force attenuates the matrix effect in plasma, which subsequently allows a clear distinction between samples extracted from patients with AD and from the NC. Moreover, this study implied that the filtration effect may become a vital step toward establishing an easy and simple plasma-based diagnosis of AD and other severe diseases.

2. Material and methods

2.1. Theory and numerical simulation

In a nonuniform electric field (E-field), the motion of molecules in a liquid is influenced by two major forces: the DEP force and the drag force. The strength of the DEP force is described by the intensity of $\nabla|E|^2$, as follows (Ramos et al., 1998):

$$F_{DEP} = 2\pi r^3 \varepsilon_m K(\omega) \bullet \nabla|E|^2 \quad (1)$$

where r represents the radius of molecules, ε_m represents the effective permittivity of liquid, and $K(\omega)$ represents the Clausius–Mossotti factor. The drag force is expressed, as follows:

$$F_{drag} = 6\pi r \eta \bullet v(t) \quad (2)$$

where η *and* v are the dynamic viscosity of liquid and flow velocity, respectively. Based on Eqs. (1) and (2), the motion and consequential position of molecules can be modified, as follows [Eq. (3)]:

$$F_{DEP} - F_{drag} = m \bullet a(t) \quad (3)$$

Finite-element models of the DEP experiments were created using the alternate current/direct current (AC/DC) module of COMSOL Multiphysics software 5.2 (COMSOL Inc., Burlington, MA, USA). To confirm the value of $\nabla|E|^2$ around the electrodes at the IMEs, 5-μm wide and 150-nm thick platinum electrodes with 5-μm wide gaps between the electrodes were modified.

2.2. Fabrication and surface functionalization of the IMEs

The IME sensor was produced via a standard micro-electro-mechanical system (MEMS) process on a 4-in. silicon (Si) wafer. The sensor was comprised 30 pairs of microelectrode fingers (spacing, 5 μm; length, 300 μm). The fabrication process is depicted in Fig. S1 and has been described previously (Kim et al., 2016). A microsized pattern for a polydimethylsiloxane (PDMS) (Dowhitech Silicone Co. Ltd., Gyeonggi-do, Korea) microfluid channel was also fabricated via the MEMS process.

The silicon dioxide (SiO_2) surface between the IMEs was treated, based on a previously described protocol (Batteiger and Jones, 1982). The SiO_2 surface was activated with 1% (w/v) (3-aminopropyl)triethoxysilane solution (Sigma-Aldrich Inc., Gyeonggi-do, Korea), 2 mM poly(*N*-vinylpyrrolidone) in aldehyde end-group solution, 10 mM Sodium tetrahydridoborate ($NaBH_4$) (Sigma-Aldrich Inc.), and 1% (w/v) glutaraldehyde solution (Daejung Chemical and Metals Co., Ltd., Gyeonggi-do, Korea). After surface activation, the antibody was immobilized on the SiO_2 surface for reacting with the target protein. All antibodies used in the given reaction were diluted to 10 μg/mL in 1 mM PBS (Corning Korea Co., Ltd., Seoul, Korea) and were covalently reacted with the activated SiO_2 surface between IMEs for 1 h at 25 °C. The following antibodies were used: purified anti-β-amyloid, 1–16 (6E10) antibody (BioLegend Inc., San Diego, CA, USA) specifically bound to the Aβ monomer, anti-amyloid fibril (OC) antibody (Rockland Immunochemicals Inc., Pottstown, PA,USA) specifically bound to Aβ fibrils, antihuman serum albumin antibody (15C7) (Abcam PLC., Cambridge, MA, USA), and antihuman immunoglobulin G (IgG) antibody (KT131) (Abcam PLC.).

2.3. System setup and analysis

The DEP force was induced by applying a sinusoidal AC, delivered using a DG4062 Series Wave form generator (Rigol Technologies Inc., Beaverton, OR, USA; frequency range, up to 60 MHz; voltage range, up to 5 V). The function generator was connected to a pair of probes (i.e.,

pads) at the end of the IMEs. The electrode pads were also connected to an IME sensor analyzer (Cantis Inc., Gyeonggi-do, Korea). A small AC signal of 10 mV, with a sweep ranging from 10 Hz to 1 MHz, was applied to the pads for measuring the sensor's impedance. The impedance of the IME sensor was measured at 50 Hz for 3 min, and the average impedance value over 30 s, after signal saturation, was used as the output signal. To verify the basic performance of the IME sensor, the reproducibility, repeatability, and stability of the sensor were analyzed in PBS (Fig. S2).

2.4. Immunoassay

Protein stocks dissolved in distilled water were diluted using PBS buffer for detection. Proteins were diluted with 1 mg/mL standard plasma (P9523) (Sigma-Aldrich Inc.) dissolved in distilled water for the plasma-based detection. The following proteins were used: Aβ protein fragment 1–42, human serum albumin (HSA), and human serum IgG (all from Sigma-Aldrich Inc.).

Antibody-protein reactions occurred in a PDMS channel attached to the IME sensor. After immobilization, approximately 20 μL of solution containing the target protein was injected into the channel. Antibody–protein reactions took place at 25 °C for 20 min, at which time the DEP force was applied simultaneously under the appropriate conditions. After the reaction, unbound proteins were washed away using 1 mM PBS. Antibody–protein interactions were analyzed, based on the absolute impedance difference, $|\Delta Z|$, which was calculated as follows: $|\Delta Z| = |(Z_{\text{after reaction}} - Z_{\text{before reaction}})|/Z_{\text{before reaction}} \times 100$. The $Z_{\text{before reaction}}$ and $Z_{\text{after reaction}}$ values denote the average values before and after, respectively, the antibody–protein reactions.

3. Results and discussion

3.1. Matrix effect

The matrix effect is a phenomenon in which a sensor's performance such as accuracy, limit of detection (LOD), and sensitivity are deteriorated by various matrix factors in a buffer (Johansson and Hellenas, 2004). Plasma contains various matrix factors with sizes ranging from a few kilo-Daltons to several hundred kilo-Daltons (O'Neil, 2012); therefore, detecting a disease's hallmark protein is difficult. Degradation in sensor performance because of the matrix effect is a major limitation of biofluid-based detection techniques (De et al., 2009; Wu et al., 2016) (Table 1). The influence of this detrimental effect can also be evaluated by the MEF, as follows (Matuszewski et al., 2003; Wu et al., 2010):

$$A - B = \text{MEF} \times A, \tag{4}$$

where A and B represent the signal produced by specific binding of target molecules in each buffer. A is measured in a buffer containing only the target protein, and B is measured in a buffer containing various matrix factors and the target protein. Based on the MEF, Eq. (4) can be modified, as follows:

$$\text{MEF} = \frac{A - B}{A}$$

$$= 1 - \frac{B}{A}$$

3.2. Dielectrophoresis-based filtration

Owing to the inhomogeneity of an electric field, DEP can be used to manipulate biomolecules such as proteins. It determines the position of biomolecules in a given region, based on the relative strength between two forces: the motive force induced by DEP (i.e., DEP force) and the drag force caused by the movement of the biomolecules in response to the DEP force (Kim et al., 2016). If the relative strengths of the two opposing forces acting on the biomolecules are similar in the region between the electrodes, the molecules remain between the electrodes. However, if one of the two forces, especially the DEP force, is dominant, the molecules are released from the region between the electrodes. The strength of the DEP force is proportional to the size of the biomolecules so that the molecules are located in different regions, based on their type. This phenomenon is verified with the IME sensor (Fig. 1a).

In the IME sensor with inhomogeneous E-field, the DEP force assigns target molecules and matrix factors larger than the targets to different regions of the sensor (Fig. 1b). If the force is optimized to situate the target molecules in a reaction region between the electrodes, which are immobilized with specific antibodies against target molecules, the matrix factors are released from the region so that they cannot bind to the antibody. Thus, only the target molecules bind to the antibody between the IMEs—the matrix factors and target molecules are filtered by the DEP force (Fig. 1c). By the selective filtration of the target molecules and matrix factors, the probability of reaction between the target molecules and the specific antibodies immobilized in the reaction

Table 1
The matrix effect in plasma; various types of sensors have a lower performance in plasma because of the matrix effect.

Target	Sensor type	Buffer	Sensor performance
Thrombin	Aptamer-based sandwich assay with electrochemical detection (Centi et al., 2007)	PBS Serum	LOD < 0.5 nM LOD < 5 nM Sensor response decreased on average by ~80%
C-reactive protein	Electrochemical sensor (Bryan et al., 2013)	PBS with Tween-20 Blood	LOD = 176 ± 18 pM LOD = 322 pM
Human chorionic gonadotropin (hCG) and activated leukocyte cell adhesion molecule (ALCAM)	Surface plasmon resonance (SPR) sensor (Piliarik et al., 2010)	Tris, ethylenediaminetetraacetic acid (TENa) Diluted blood plasma	LOD = 7 ng/mL for ALCAM, 13 ng/mL for hCG LOD = 45 ng/mL ALCAM, 100 ng/mL for hCG
Brain natriuretic peptide	Reduced graphene oxide (rGO) field effect transistor (Lei et al., 2017)	PBS Whole blood	LOD = 100 fM LOD = 50 nM
Infliximab	Fiber-optic SPR sensor (Lu et al., 2017)	Diluted serum Diluted plasma Diluted whole blood	LOD = 1.42 ng/mL LOD = 1.00 ng/mL LOD = 1.34 ng/mL
α-Fetoprotein (AFP)	Magnetic nanoparticle-based electrochemical immunosensor (Xu et al., 2017)	PBS Whole blood	LOD = 0.072 ng/mL Evaluated from the response to 20 ng/mL AFP
Glucose	Dual enzyme-inorganic hybrid nanoflower incorporated microfluidic paper-based analytic device (Zhu et al., 2017)	Ultrapure water Whole blood	LOD = 25 μM Detection of glucose in the whole blood with concentrations of 2.8–14.4 mM

PBS, phosphate-buffered saline; LOD, limit of detection.

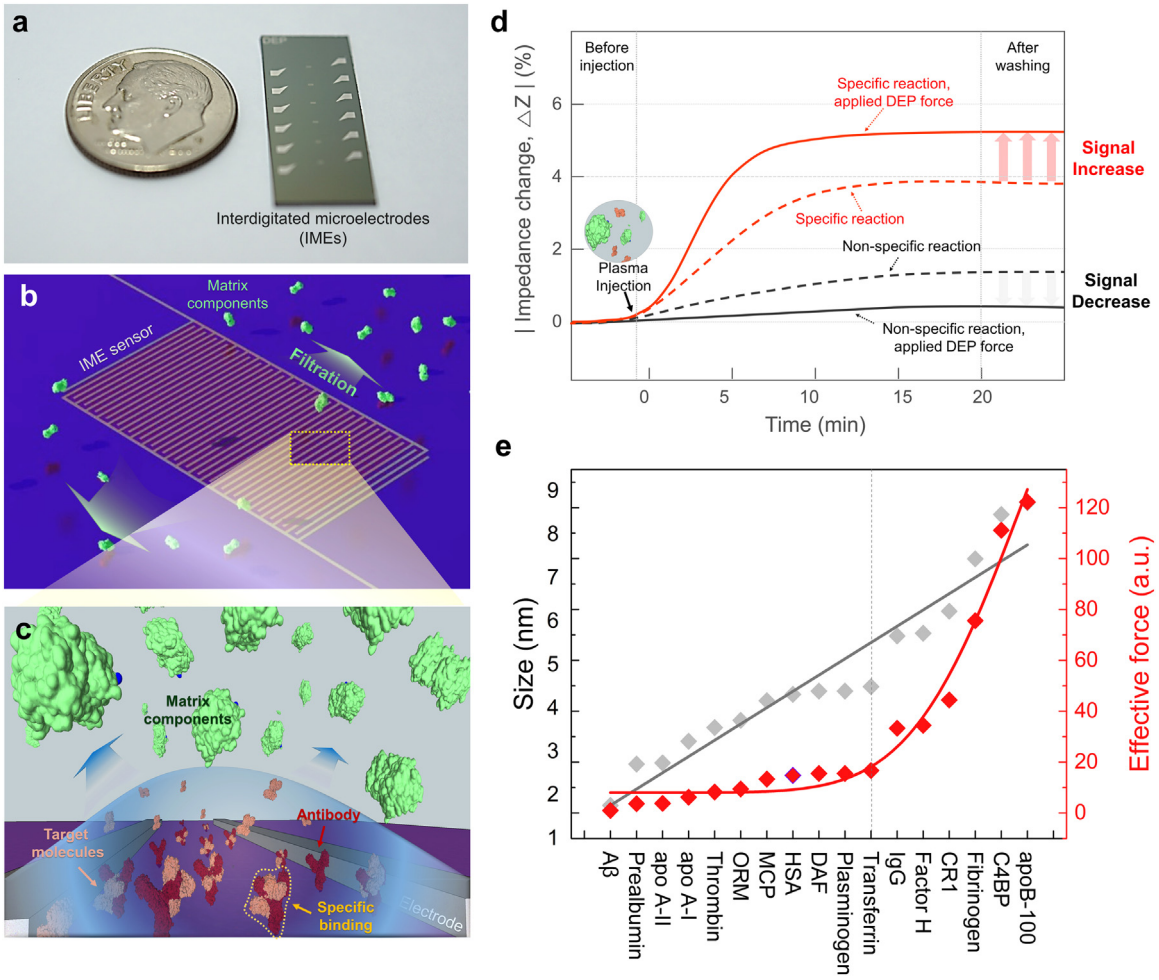

Fig. 1. Plasma-based biomolecule quantification method. (a) A chip comprising six arrays of interdigitated microelectrode (IME) sensors for the plasma-based quantification of biomolecules. (b) The IME sensor can detect a target molecule effectively by the filtration effect caused by the dielectrophoresis (DEP) force. (c) The DEP force expels from the sensing region nonspecifically absorbed matrix factors that are larger than the target molecules. The target molecules remain between the electrodes in the sensing region and, consequently, only the remaining molecules are quantified by the IMEs. (d) The filtration effect decreases the impedance change of the IME sensor because of specific binding, while increasing the change owing to the specific binding of target molecules. The solid and dashed lines represent the impedance change in the reaction conditions with and without the filtration effect, respectively. The red and black lines indicate the impedance changes due to specific binding of target molecules and nonspecific binding of matrix factors, respectively. (e) Plasma consists of molecules of various sizes. These molecules are influenced by different forces. The intensity ratio of each force was calculated, based on the intensity of the force applied to the amyloid beta (Aβ) monomer. C4BP, complement component 4 binding protein; CR1, complement receptor 1; DAF, decay-accelerating factor; HSA, human serum albumin; IgG, immunoglobulin G; MCP, monocyte chemoattractant protein; ORM, orsomucoid; apo A-I, apolipoprotein A1; apo A-II, apolipoprotein A2.

region increases. As a consequence, the impedance change by their specific binding increases, whereas the impedance change by non-specific binding of matrix factors decreases (Fig. 1d). In our study, we define this phenomenon as the filtration effect.

For quantification of plasma Aβ monomers, only the Aβ monomer should be in the reaction region and various matrix factors should be filtered from the region by an optimized DEP force, which situates the Aβ monomers in the reaction region. Previous studies have indicated that an E-field intensity of approximately 10^{19} V^2/m^3 is required to concentrate the Aβ monomer (Kim et al., 2016). The DEP force is proportional to the cube of a protein's size; therefore, proteins larger than the Aβ monomer are exposed to a relatively stronger force than the Aβ monomer in an E-field of the same intensity (Bieschke et al., 2011). Differences in these effective forces enable protein filtration. The size can be calculated using Erickson's equation (Erickson, 2009). Based on intensity of the optimized DEP force on the Aβ monomer, the relative intensities of the DEP force that affect various matrix factors in plasma are expressed as the effective force (i.e., intensity ratios for the optimized force on the Aβ monomer) (Fig. 1e). For protein sizes below 3 nm, the effective force fell below 20 a.u. (transferrin), whereas the force rapidly increased up to 120 a.u. when applied to proteins larger than transferrin. The different intensities of the effective force obtained for various matrix factors signified that Aβ monomers are sufficiently filtered from the plasma's matrix factors.

3.3. Verification of the filtration effect

In general, the sensitivity of a sensor is its ability to detect a signal change, based on the concentration of target molecules; it inevitably decreases in plasma containing various matrix factors that interfere with the specific binding of target molecules. Therefore, the efficiency of the filtration effect is evaluated by the sensitivity and MEF, which increase and decrease, respectively, with highly efficient filtration.

The sensitivity of Aβ monomer quantification was lower for plasma than for PBS (Fig. 2a). To ascertain the influence of the matrix on sensor sensitivity, Aβ monomer was quantified at concentrations ranging from 100 fg/mL to 100 pg/mL (Fig. S3). Impedance changes were approximately 1.19 ± 0.38 in PBS containing the Aβ monomer and 0.55 ± 0.07 in plasma containing various matrix factors and the Aβ monomer (the values are expressed as the mean ± the standard

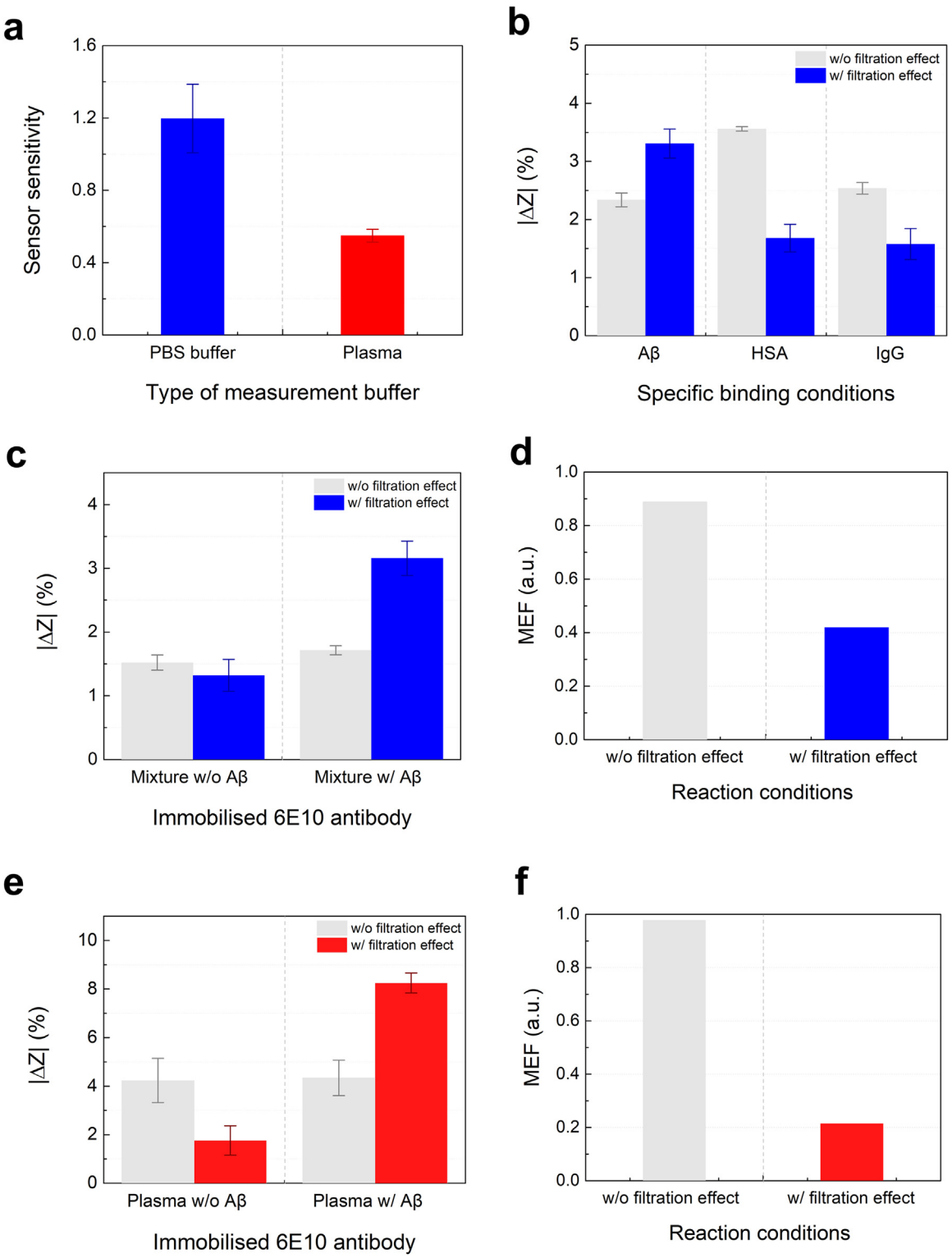

Fig. 2. Verification of the filtration effect due to the dielectrophoresis (DEP) force. The matrix effect causes the decline of the sensor's performance can be decreased by the filtration effect of DEP force. (a) Decreased performance in the interdigitated microelectrode (IME) due to the matrix effect was confirmed by assessing sensor sensitivity in two types of reactions: phosphate-buffered saline-based and plasma-based. (b) Impedance changes due to specific binding between various molecules (amyloid beta [Aβ] monomer, human serum albumin [HSA], and immunoglobulin G [IgG]) and their specific antibodies, and (c) due to two types of binding with 6E10 in mixture without (w/o) and with (w/) Aβ monomer were measured according to the effect of filtration. (d) The matrix effect factor (MEF) value for the two types of reaction conditions were calculated. The value decreased due to the filtration effect. (e) The impedance changes due to two types of binding with 6E10 in plasma without and with the Aβ monomer were also measured, based on the filtration effects. (f) The decreased MEF value due to filtration was verified.

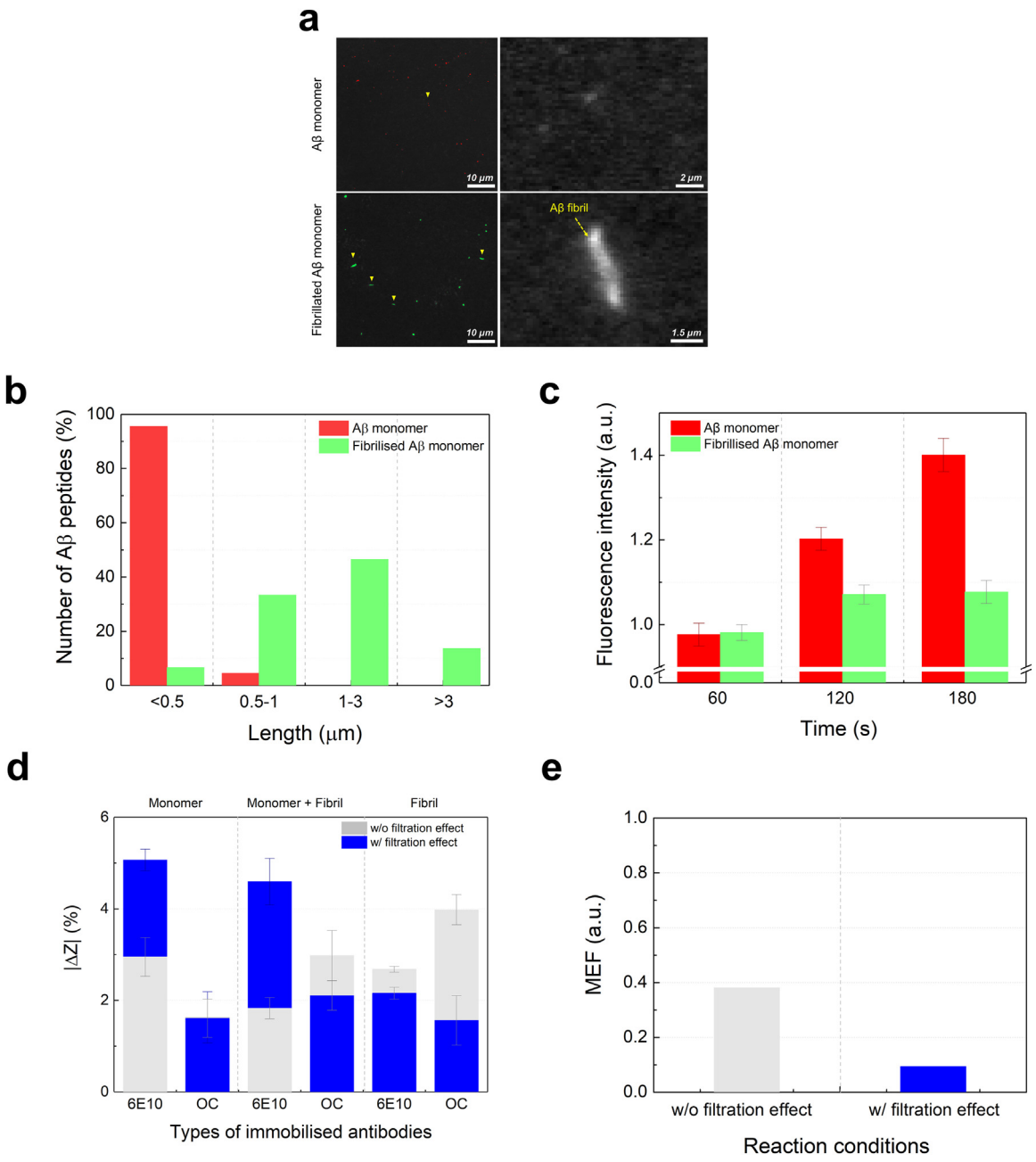

Fig. 3. Demonstration of the filtration effect, based on the heterogeneity of beta-amyloid (Aβ). The Aβ monomer can be fibrillized, depending on the incubation time. (a) The Aβ monomer and the fibrillized Aβ after incubation. (b) The ratio of monomeric and fibrillar Aβ in two types of buffers, based on the corresponding range of length, was analyzed. The fibrillized Aβ level indicates whether the Aβ monomer in the buffer is undergoing fibrillization. (c) The fluorescence intensities of each Aβ monomer and fibril were analyzed, based on the duration of the applied dielectrophoresis (DEP) force. (d) The impedance change during Aβ detection in 1 mM phosphate-buffered saline is measured with (w/) and without (w/o) the filtration effect. The reaction between two types of antibodies and three types of solutions causes diverse changes in impedance, based on their binding caused by the DEP force. (e) Matrix effect factors are calculated, based on the filtration effects.

deviation). These results demonstrated that the sensitivity of the sensor was reduced by 54.33% because of the matrix effect in plasma, compared with PBS.

To confirm the filtration effect, an immunoassay of the specific binding of three types of biomolecules was performed under two binding conditions: with and without the filtration effect (Fig. 2b). The molecules were the Aβ monomer; the plasma matrix proteins HAS and immunoglobulin G (IgG); and T, which is an abundant matrix factor in plasma. The concentration of each protein in PBS were the same at 10 pg/mL (Kratochwil et al., 2002). The reaction between the biomolecules and their specific antibody disturbs the E-field formed between the electrodes. Therefore, the impedance change increases as the reaction between the molecules and antibody increases. The impedance change caused by the specific binding of the Aβ monomer was approximately 2.34% ± 0.12% (n = 4), and improved to approximately 3.21% ± 0.27% (n = 3) by the filtration effect. By contrast, filtration reduced the impedance change for HSA and IgG. The impedance changes because of the binding of HSA and IgG were approximately 3.56% ± 0.04% (n = 3) and 2.53% ± 0.10% (n = 3) without filtration, and approximately 1.68% ± 0.24% (n = 3) and 1.58% ± 0.27% (n = 3) with the filtration effect. These results indicated that the HSA and IgG were expelled from the reaction region by the filtration effect, which resulted in the decreased reaction probability of HSA and IgG. The impedance changes because of nonspecific binding between

antibody and biomolecules were not associated with the filtration effect (Fig. S4).

The filtration effect was further verified in a buffer containing three or more different biomolecules. The surface of the sensor was functionalized only with the 6E10 antibody, and two types of mixing buffer were used: one buffer consisted of HSA and IgG acting as the matrix factors and the other buffer consisted of Aβ monomer, HAS, and IgG (Fig. 2c).

The concentrations of the Aβ monomer, HSA, and IgG in PBS were 10 pg/mL each, and the conditions were the same as those presented in Fig. 2b. In a buffer consisting only of matrix factors, the absorption between the immobilized antibody and matrix factors was suppressed by the filtration effect, and the impedance change was decreased. The changes were approximately 1.52% ± 0.10% (n = 5) and 1.32% ± 0.15% (n = 4) without and with the filtration effect, respectively. The impedance change in the solution containing the Aβ monomer, HSA, and IgG was enhanced by the filtration effect; the change was approximately 1.71% ± 0.07% (n = 12) and 3.16 ± 0.60% (n = 12) without and with the effect, respectively. Thus, the MEF values for detecting the Aβ monomer in the matrix buffer containing HSA and IgG were reduced by approximately 52.87% (from 0.89 to 0.42) by the filtration effect. The matrix effect was alleviated by effectively filtering HSA and IgG (Fig. 2d). Furthermore, the findings implied that the matrix effect was much more effective in a complicated buffer containing various matrix factors such as plasma and urine.

Plasma contains various types of matrix factors that interfere with the specific binding of the Aβ monomer. Therefore, the actual values of detection sensitivity and accuracy measured in plasma should be lower than those measured in PBS, whereas filtration should be stronger in plasma than in PBS. To demonstrate the filtration effect in plasma, the impedance changes occurring because of the reaction between the 6E10 antibody and the biomolecules in two types of plasma (1 mg/mL) with and without the Aβ monomer (10 pg/mL) were measured (Fig. 2e). The applied voltage and frequency conditions for generating the filtration effect were also the same as previously described. In plasma without the Aβ monomer, filtration decreased the impedance change from approximately 4.24% ± 0.91% (n = 12) to 1.76% ± 0.60% (n = 12). In plasma containing Aβ monomers, the filtration effect enhanced the change in impedance, and the changes were approximately 4.34% ± 0.73% (n = 9) and 8.25% ± 0.41% (n = 12) without and with the filtration effect, respectively.

Quantitative analysis was also conducted by using the respective values of the MEF to subtract the impedance change caused by the absorption from the impedance change measured for the plasma containing the Aβ monomer (Fig. 2f). The filtration effect significantly lowered the MEF value from approximately 0.97 to 0.21. The decreased ratio of the MEF caused by filtration was approximately 78.12%, which was higher than the ratio measured in PBS. These findings demonstrated that the filtration effect is more potent in plasma.

3.4. The filtration effect, based on the heterogeneity of Aβ

The status, progression, and prognosis of AD can be determined from the level of Aβ, especially Aβ monomers; therefore, it is important to filter the monomeric Aβ from among the various types of Aβs and quantify the filtrated Aβ monomers in plasma. To verify the detectability of Aβ monomers, based on their heterogeneity, various structures of the Aβs were synthesized, and the impedance change by the immune-reaction was analyzed in the presence of the filtration effect. A fibrillogenesis-based process was used to control the Aβ structure, which allowed the Aβ monomers to develop into larger and more complex Aβ fibrils over time. Changes in structure were confirmed by measuring the change in impedance for reactions involving the monomer-specific antibody 6E10 and fibril-specific antibody OC. Furthermore, the change in structure was verified via photo-induced cross-linking of unmodified proteins. The structure of Aβ before and after fibrillogenesis was observed using fluorescence microscopy (Figs. 3a and S5). The details of the information are described in the Supplement. In these images, Aβ monomers appeared blurry because of their small size, whereas wire-shaped fibrils were clearly visible; this finding was similar to the findings reported in previous studies (Bieschke et al., 2011).

After fibrillogenesis, most Aβ monomers were below 0.5 μm in length, whereas only approximately 4.51% of the Aβ monomers ranged 0.5–1.0 μm in length. By contrast, most Aβ fibrils were greater than 0.5 μm in length (Fig. 3b). The percentage of Aβ fibrils in each length range was as follows: less than 5 μm, approximately 6.58%; 0.5–1.0 μm, approximately 33.33%; 1.0–3.0 μm, approximately 46.49%; and more than 3 μm, 13.61%. The findings demonstrated that Aβ fibrils were subjected to an effective force that was more than six times larger than the force applied to Aβ monomers in the same DEP condition; therefore, only Aβ monomers remained in the reaction region.

The expected effective force was deduced, based on differences in length only; the actual effective force applied to the fibrils may have been greater (1) because the actual size of Aβ monomers is smaller than the observed value (Giuffrida et al., 2009) and (2) because of the observed increase in Aβ fibril radius. The difference in the effective force permitted the filtration of Aβ monomers and fibrils. This action was confirmed, based on the intensity of fluorescence relative to the length of time of the DEP force (Fig. 3c). The intensity of fluorescence within the reaction region was measured between IMEs. Fluorescence intensities were expressed relative to the intensity measured in the reference condition (i.e., DEP force duration = 0 s). The intensities of Aβ monomers were approximately 0.98 ± 0.03, 1.20 ± 0.03, and 1.40 ± 0.04, whereas those of Aβ fibrils were approximately 0.98 ± 0.02, 1.07 ± 0.02, and 1.08 ± 0.03 at 60 s, 120 s, and 180 s, respectively. These findings demonstrated that Aβ monomers were situated in the reaction region because of the filtration effect of the DEP force, whereas the Aβ fibrils were not in this region.

The filtration effect was also verified by measuring the impedance change in various reaction conditions using two types of antibodies (6E10 and OC) and three types of target solutions (Fig. 3d). Target solutions were chosen, based on the volume ratio of the Aβ fibril and Aβ monomer solutions (V_f/V_m), and expressed as monomer (V_f/V_m = 0/1), monomer + fibril (V_f/V_m = 1/1), and fibril (V_f/V_m = 1/0). Greater changes in impedance associated with Aβ monomer binding were observed in the condition with the filtration effect than in the control condition without the filtration effect (i.e., 6E10 antibody in the monomer region). Greater changes in impedance associated with Aβ fibril binding occurred under the conditions without the filtration effect (i.e., OC antibody in fibril region).

Changes in specific binding of the Aβ monomers were approximately 2.95% ± 0.42% (n = 7) and 5.07% ± 0.24% (n = 6) without and with the filtration effect, respectively. Changes in specific binding of Aβ fibrils were approximately 3.98% ± 0.33% (n = 8) and 1.56% ± 0.54% (n = 7) without and with the effect, respectively. These results indicated that specific binding of antibodies to proteins was influenced by the filtration effect.

By contrast, the filtration effect was insignificant in the nonspecific binding conditions (i.e., Aβ monomer to OC antibody in the monomer region; Aβ fibril to 6E10 antibody in the fibril region). Changes in impedance for Aβ monomer reactions were approximately 1.63% ± 0.56% (n = 6) and 1.61% ± 0.42% (n = 5) without and with the filtration effect, respectively, whereas changes for Aβ fibril reactions were approximately 2.68% ± 0.07% (n = 6) and 2.15% ± 0.13% (n = 5) without and with the filtration effect, respectively. The filtration effect also occurred in a buffer containing both Aβ monomers and fibrils. The effect was quantified by calculating the MEF, and was confirmed by measuring the change in impedance in the monomer + fibril region. An approximately 2.5-fold increase in impedance change due to the DEP force occurred for immobilized 6E10 antibody: approximately 1.83% ± 0.46% (n = 6) and

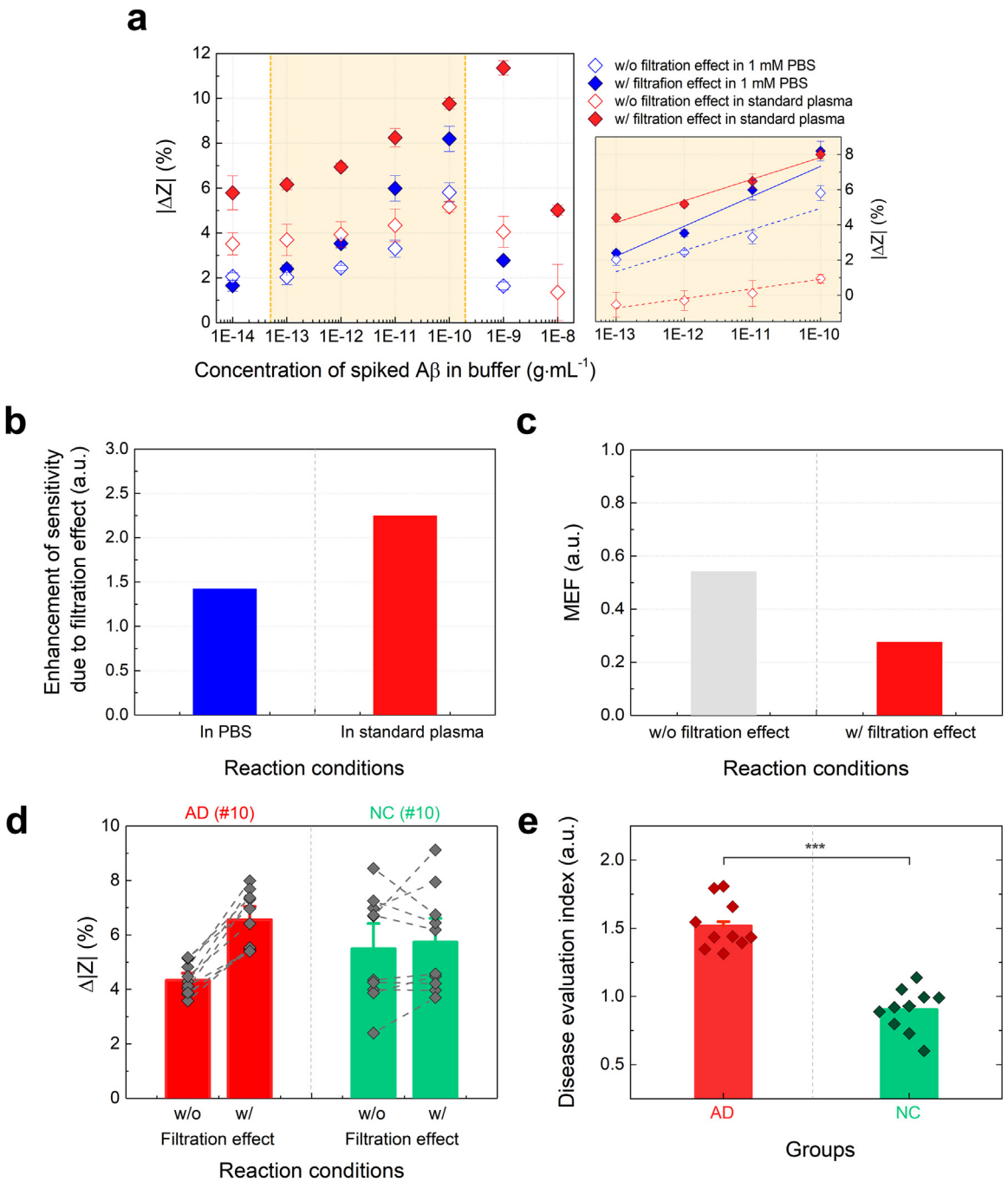

Fig. 4. Diagnosis of Alzheimer's disease (AD). (a) The sensitivities are improved by the filtration effect in PBS-based detection and plasma-based detection. (b) Enhancement of the sensitivity measured in standard plasma versus that measured in 1 mM phosphate-buffered saline (PBS) buffer. (c) Decreased matrix effect factor (i.e., calculated) produced by filtration. (d) Impedance changes due to the reaction of the 6E10 antibody with plasma extracted from patients with AD (n = 10) or normal controls (NCs) (n = 10), measured in detection with (w/) or without (w/o) filtration. The scatter plots indicate the impedance value of patients and columns show the average value of the impedance values. (e) Dielectrophoresis enhancement factors, calculated for AD plasma and NC plasma. Significant group differences are indicated by P-values (one-way analysis of variance [ANOVA]) and by asterisks: *p < 0.05, **p < 0.01, ***p < 0.001.

4.59% ± 0.51% (n = 4) without and with the filtration effect, respectively. A decrease in the impedance change due to the filtration effect occurred for immobilized OC antibody: approximately 2.98% ± 0.55% (n = 6) without the filtration effect and 2.11% ± 0.64% (n = 8) with the effect.

Based on these values, we calculated the MEF by using Eq. (2). The MEF values were approximately 0.38 and 0.09 without and with the filtration effect, respectively (Fig. 3e). An approximately 75.43% decrease in the MEF indicated that Aβ can be sufficiently sorted structurally by the filtration effect.

3.5. The filtration effect in PBS and standard plasma and patient plasma for detecting Aβ

First, the impedance change by specific binding of Aβ monomer at various concentrations was measured in two types of buffer: PBS and standard plasma (1 mg/mL) without and with the filtration effect (Fig. 4a). The concentration of Aβ monomer in the buffer ranged from 10 fg/mL to 1 ng/mL. The impedance change measured in PBS without the filtration effect was approximately 2.06% ± 0.17% (n = 6), 2.03% ± 0.33% (n = 5), 2.44% ± 0.11% (n = 5), 3.29% ± 0.38%

(n = 6), 5.81% ± 0.43% (n = 5), and 1.63% ± 0.17% (n = 4), based on the concentration of the Aβ monomer. The change was improved by the filtration effect by approximately 1.65% ± 0.25% (n = 6), 2.40% ± 0.17% (n = 6), 3.53% ± 0.19% (n = 4), 5.99% ± 0.57% (n = 4), 8.19% ± 0.56% (n = 5), and 2.78% ± 0.05% (n = 4), based on the concentration of the Aβ monomer. An enhancement in the impedance change caused by the filtration effect also occurred when detecting Aβ monomer in plasma. The magnitude of the impedance change improved by at least 2%.

The impedance change measured in plasma without the filtration effect was approximately 3.52% ± 0.49% (n = 8), 3.69% ± 0.70% (n = 13), 3.94% ± 0.56% (n = 9), 4.34% ± 0.73% (n = 9), 5.17% ± 0.25% (n = 4), and 4.05% ± 0.69% (n = 6). The filtration effect improved the values to approximately 5.79% ± 0.76% (n = 7), 6.16% ± 0.23% (n = 8), 6.94% ± 0.17% (n = 5), 8.25% ± 0.41% (n = 12), 9.77% ± 0.25% (n = 12), and 11.36% ± 0.32% (n = 10), respectively, for each Aβ monomer concentration.

In addition, the impedance variations that occurred because of nonspecific binding were analyzed to demonstrate the LOD of the sensor (Fig. S6). These impedance variations, which were considered the noise signal, were approximately 2.04% ± 0.14% (n = 6) and 1.41% ± 0.10% (n = 7) in PBS, and approximately 4.24% ± 0.60% (n = 6) and 1.76% ± 0.30% (n = 7) in plasma, based on the filtration effect. These findings indicated that the filtration effect lowered the LOD in PBS from 100 fg/mL to 10 fg/mL and the LOD in plasma from 10 pg/mL to 100 fg/mL. The fact that the LOD value was more greater in plasma than in PBS indicated that the filtration effect was more efficient in plasma than in PBS. The efficiency of the filtration effect was also confirmed by the enhanced sensitivity values in each buffer. These results demonstrated a linear correlation between the concentration of Aβ monomer and normalized impedance change, based on linear regression analysis. (The linear equation is y = Intercept + Slope × x; the value of the slope signifies the sensitivity of the sensor for Aβ monomer reaction.) The values verified the conditions without and with the filtration effect were approximately 1.19 ± 0.38 and 1.70 ± 0.31, respectively, in PBS buffer and were approximately 0.55 ± 0.07 and 1.23 ± 0.14, respectively, in plasma.

Various matrix factors in plasma hindered the specific binding of Aβ monomer to 6E10 antibody. Therefore, the sensitivity values verified in plasma were reduced, regardless of the filtration effect. However, the enhanced ratio of sensitivity due to the filtration effect measured in plasma was higher than that measured in PBS; the ratios were approximately 1.42 and 2.25, respectively (Fig. 4b). Based on their sensitivities, the MEF values were calculated to be approximately 0.54 and 0.28 in the reaction conditions without and with the filtration effect, respectively (Fig. 4c). Approximately 49.32% of the MEF was decreased. This finding indicated that the matrix effect was effectively alleviated by the filtration effect.

The impedance change due to the filtration effect was analyzed in plasma samples drawn from patients with AD and from the NCs (for each group, n = 10). The average impedance change in the AD patients' plasma was approximately 4.33% ± 0.26% without filtration and 6.56% ± 0.49% with filtration (Fig. 4d). By contrast, the average impedance change was approximately 5.50% ± 0.93% and 5.74% ± 0.87% without and with filtration, respectively, of the plasma of the NCs. These impedance changes in the two plasma types showed a significant tendency of differential the filtration effect. When impedance changes were tracked over two reaction conditions—without or with the filtration effect—the changes in impedance increased after the filtration effect in the AD patients' plasma, whereas most changes in impedance decreased after the filtration effect in NC plasma. This finding was verified by calculating a disease evaluation index that removed the matrix effect (Fig. 4e). In Fig. 4e, the values of impedance change in the AD and NC plasma are depicted as red and dark green diamonds, respectively, and the average value of these changes are depicted in a column. The index represents the ratio of impedance change between conditions without and with the filtration effect. A value greater than "1" signifies that Aβ reacted more with the specific antibody because of the filtration effect, which decreased the matrix effect. Thus, the results indicated that Aβ in the AD patients plasma was detected more efficiently because the matrix effect was alleviated by the filtration effect. By contrast, Aβ in NC plasma was only slightly affected by the filtration effect because the NCs had low levels of Aβ. The average values of the disease evaluation index were approximately 1.52 ± 0.03 and 0.90 ± 0.03 in the plasma of AD patients and the NCs, respectively ($p < 0.001$). These findings indicated that the filtration effect caused by the DEP force attenuates the matrix effect in plasma, and subsequently allows a clear distinction between the plasma of patients with AD and NCs. Moreover, this study indicated that the filtration effect may become a vital step toward an easy and simple plasma-based diagnosis of AD and other severe diseases.

4. Conclusion

In this study, we developed a novel method of protein quantification in a biofluid by using the filtration effect induced by the DEP force and demonstrated the potential application of this method for the early diagnosis of AD. First, the optimized force required to filter the Aβ monomer was calculated by simulation and applied to detect the Aβ monomer for verifying the filtration effect. As a result, the filtration effect increased the impedance change because of the specific binding of the Aβ, whereas the filtration effect decreased the impedance change because of nonspecific binding. Based on the impedance change, the MEF value was calculated. We verified that all values decreased. Second, Aβ monomers were quantified in PBS and in standard plasma, and the MEF values were consequently calculated as approximately 0.54 and 0.28 without and with the filtration effect, respectively. The findings indicated that the filtration effect facilitates highly selective quantification of the Aβ monomer, regardless of the buffer type.

We also demonstrated that the filtration effect increased changes in impedance in AD plasma, whereas most values decreased in the NC plasma samples. These changes were verified with the disease evaluation index, which removed the matrix effect, based on the average values of the index in the NC and AD plasma samples. The index values were approximately 1.52 ± 0.03 and 0.90 ± 0.03, respectively ($p < 0.00001$). These findings indicated that the filtration effect can overcome the limits of Aβ monomer quantification in real plasma by alleviating the matrix effect, and can allow NC and AD plasma samples to be distinguished. Our research demonstrated the possibility of simply and easily diagnosing AD based on thelevel of Aβ protein in the plasma and indicated that the filtration effect can be utilized for making a plasma-based diagnosis of other severe diseases.

Acknowledgements

This work was financially supported by the Korea Health Industry Development Institute (KHIDI, Republic of Korea; grant no. HI14C3319), National Research Foundation of Korea (NRF, Republic of Korea, grant no. NRF-2017R1C1B5075822), and Korea Institute of Industrial Technology (KITECH, Republic of Korea, Project no. EO170047).

Credit author statement

H.J.K., J.K. and K.S.H. conceived and designed the experiments. H.J.K, and D.P. performed most of the experiments, contributed to experimental design, data analysis and writing. S.Y.B, S.H.Y. and Y.K. performed biological experiment and served the validation. S.M.L. supplied resources of clinical samples in this study. J.K. and K.S.H. designed and supervised the study, analyzed the data, and wrote the manuscript. All authors discussed the results and commented on the manuscript.

Declaration of interests

None.

Appendix A. Supporting information

Supplementary data associated with this article can be found in the online version at doi:10.1016/j.bios.2018.12.046

References

Al-Mashikhi, S.A., Nakai, S., 1988. J. Dairy Sci. 71, 1756–1763.
Arya, R.C., Wander, G.S., Gupta, P., 2011. J. Anaesthesiol. Clin. Pharmacol. 27, 278–284.
Batteiger, B., Jones, R.B., 1982. J. Immunol. Methods 55, 297–307.
Bieschke, J., Herbst, M., Wiglenda, T., Friedrich, R.P., Boeddrich, A., Schiele, F., Kleckers, D., Lopez del Amo, J.M., Grüning, B.A., Wang, Q., Schmidt, M.R., Lurz, R., Anwyl, R., Schnoegl, S., Fändrich, M., Frank, R.F., Reif, B., Günther, S., Walsh, D.M., Wanker, E.E., 2011. Nat. Chem. Biol. 93–101.
Bryan, T., Luo, X., Bueno, P.R., Davis, J.J., 2013. Biosens. Bioelectron. 39, 94–98.
Chuang, C.H., Du, Y.C., Wu, T.F., Chen, C.H., Lee, D.H., Chen, S.M., Huang, T.C., Wu, H.P., Shaikh, M.O., 2016. Biosens. Bioelectron. 84, 126–132.
Centi, S., Tombelli, S., Minunni, M., Mascini, M., 2007. Anal. Chem. 79, 1466–1473.
Choi, S., Song, S., Choi, C., Park, J.K., 2007. Lab. Chip 7, 1532–1538.
De, M., Rana, S., Akpinar, H., Miranda, O.R., Arvizo, R.R., Bunz, U.H., Rotello, V.M., 2009. Nat. Chem. 1, 461–465.
Dobson, C.M., 2003. Nature 426, 884–890.
Du, H., Strohsahl, C.M., Camera, J., Miller, B.L., Krauss, T.D., 2005. J. Am. Chem. Soc. 127, 7932–7940.
Erickson, H.P., 2009. Biol. Proced. Online 11, 32–51.
Gao, Z., Xia, H., Zauberman, J., Tomaiuolo, M., Ping, J., Zhang, Q., Ducos, P., Ye, H., Wang, S., Yang, X., Lubna, F., Luo, Z., Ren, L., Johnson, A.T.C., 2018. Nano Lett. 18, 3509–3515.
Giuffrida, M.L., Caraci, F., Pignataro, B., Cataldo, S., Bona, P.D., Bruno, V., Molinaro, G., Pappalardo, G., Messina, A., Palmigiano, A., Garozzo, D., Nicoletti, F., Rizzarelli, E., Copani, A., 2009. J. Neurosci. 29, 10582–10587.
Gorkin, R., Park, J., Siegrist, J., Amasia, M., Lee, B.S., Park, J.-M., Kim, J., Kim, H., Madou, M., Cho, Y.-K., 2010. Lab. Chip 10, 1758–1773.
Hardy, J., Selkoe, D.J., 2002. Science 297, 353–356.
Herr, A.E., Hatch, A.V., Throchmorton, D.J., Tran, H.M., Brennan, J.S., Giannobile, W.V., Singh, A.K., 2007. Proc. Natl. Acad. Sci. USA 104, 5268–5273.
Jeyachandran, Y.L., Mielczarski, J.A., Mielczarski, E., Rai, B., 2010. J. Colloid Interface Sci. 341, 136–142.
Johansson, M.A., Hellenas, K.E., 2004. Analyst 129, 438–442.
Kim, H.J., Kim, J., Yoo, Y.K., Lee, J.H., Park, J.H., Hwang, K.S., 2016. Biosens. Bioelectron. 85, 977–985.
Kratochwil, N.A., Huber, W., Muller, F., Kansy, M., Gerber, P.R., 2002. Biochem. Pharmacol. 64, 1355–1374.
Lei, Y.M., Xiao, M.-M., Li, Y.-T., Zhang, H., Zhang, Z.-Y., Zhang, G.-J., 2017. Biosens. Bioelectron. 91, 1–7.
Lu, J., Spasic, D., Delport, F., Stappen, T.V., Detrez, I., Daems, D., Vermeire, S., Gils, A., Lammertyn, J., 2017. Anal. Chem. 89, 3666–3671.
Matuszewski, B.K., Constanzer, M.L., Chavez-Eng, C.M., 2003. Anal. Chem. 75, 3019–3030.
Murphy, M.P., LeVine 3rd., H., 2010. J. Alzheimers Dis. 19, 311–323.
O'Neil, D., 2012. Blood Components. Palomar College, San Marcos, CA, USA.
Piliarik, M., Bockova, M., Homola, J., 2010. Biosens. Bioelectron. 26, 1656–1661.
Ramos, A., Morgan, H., Green, N.G., Castellanos, A., 1998. J. Phys. D Appl. Phys. 31, 2338.
Rifai, N., Gillette, M.A., Carr, S.A., 2006. Nat. Biotechnol. 24, 971–983.
Ross, C.A., Poirier, M.A., 2004. Nat. Med. 10, S10–S17.
Salazar, S.V., Strittmatter, S.M., 2017. Biochem. Biophys. Res. Commun. 483, 1143–1147.
Sharma, A., Han, C.-H., Jang, J., 2016. Biosens. Bioelectron. 82, 78–84.
Soleymani, L., Fang, Z., Lam, B., Bin, X., Vasilyeva, E., Ross, A.J., Sargent, E.H., Kelley, S.O., 2011. ACS Nano 5, 3360–3366.
Tripathi, N., Singh, P., Luxami, V., Mahajan, D., Kumar, S., 2018. Sens. Actuators B Chem. 270, 552–561.
Wen, Y., Pei, H., Shen, Y., Xi, J., Lin, M., Lu, N., Shen, X., Li, J., Fan, C., 2012. Sci. Rep. 2, 867.
Wu, C., Duan, J., Liu, T., Smith, R.D., Qian, W.J., 2016. J. Chromatogr. B Anal. Technol. Biomed. Life Sci. 1021, 57–68.
Wu, J.M., Qian, X.Q., Yang, Z.G., Zhang, L., 2010. J. Chromatogr. A 1217, 1471–1475.
Xu, T., Chi, B., Wu, F., Ma, S., Zhan, S., Yi, M., Xu, H., Mao, C., 2017. Biosens. Bioelectron. 95, 87–93.
Zhu, X., Huang, J., Liu, J., Zhang, H., Jiang, J., Yu, R., 2017. Nanoscale 9, 5658–5663.